STRUCTURE AND ELECTRONIC EFFECTS OF COBALT FERRITES, $Co_xFe_{3-x}O_4$, ON CATALYTIC DECOMPOSITION OF ISOPROPANOL

Khalf-Alla M. ABD EL-SALAAM, Abd El-Aziz A. SAID*, Ahmed M. EL-AWAD, Ehsan A. HASSAN and Mohamed M. M. ABD EL-WAHAB

Chemistry Department,
Faculty of Science, Assiut University, 715 16 Assiut, Egypt

Received December 14, 1993
Accepted May 10, 1994

The cobalt–ferrite spinel oxides $Co_xFe_{3-x}O_4$ ($O < x < 3$) have been prepared by coprecipitation. Their structures were characterized by DTA, X-ray diffraction and IR spectra, and their surface properties were determined from nitrogen adsorption isotherms at –196 °C. Conductance of all the compositions was studied with and without isopropanol. The variation of E_σ values was discussed in terms of oxide semiconducting properties and of ion distribution in the octahedral-tetrahedral sites of the spinel structures. The catalytic decomposition of isopropanol at 325 °C in a flow system allowed to conclude that the inverse spinels formed in the iron-rich region are active and selective sites for acetone formation, in contrast to the inverse spinels formed in the cobalt-rich region. On the other hand, the region of normal spinels showed low activity and selectivity to acetone formation. Correlations between the composition and electronic and catalytic properties of the catalysts are reported.

Surface and bulk properties of ferrites have implications in several fields such as catalysis and electrocatalysis, corrosion of metal alloys, as well as electronic applications. The interesting physical and chemical properties of spinel ferrites arise from their activity to distribute cations among available tetrahedral (t) and octahedral (o) sites[1]. Cobalt–ferrite spinels are of considerable industrial interest due to their catalytic activity[2–5], structural stability, long life-time and resistance to sintering. The high activity of the oxides was ascribed to the presence of Co^{2+} on octahedral sites which initiated a cyclic electron transfer[6]. Stoichiometric $CoFe_2O_4$ contains only Co^{2+} and Fe^{3+}. Semiconducting properties of $Co_xFe_{3-x}O_4$ have been investigated with $x < 1$; the excess Fe^{2+} acts as an electron donor, causing n-type semiconductivity. When $x > 1$, Co^{3+} acts as an electron acceptor, causing p-type semiconductivity. However, it was already found that the wide variation of x in the cobalt–iron spinel system leads to a drastic change of its catalytic and electrical properties. However, little attention has been paid to the cata-

* The author to whom correspondence should be addressed.

lytic activity and electrical conductivity in relation to the surface structure and texture of $Co_xFe_{3-x}O_4$ in the $0 \leq x \leq 3$ range.

The present paper reports the results of electrical conductivity measurements and of the decomposition of isopropanol on $Co_xFe_{3-x}O_4$ system. The physico-chemical properties of solid cobalt ferrites were characterized by DTA, IR spectra and XRD techniques. The surface characteristics of various samples were obtained by N_2 adsorption isotherms conducted at −196 °C. The catalytic activity and selectivity of different catalysts were tested using isopropanol decomposition. Finally, semiconducting properties of the catalysts were determined both in the presence and absence of the above alcohol.

EXPERIMENTAL

Materials

Analar grade chemicals were used. Mixed samples of iron and cobalt hydroxides (with the Co^{2+} mol content x = 0.0, 0.2, 0.4, 0.6, 0.8, 1.0, 1.5, 2.0, 2.2, 2.4, 2.6, 2.8 and 3.0) were prepared by reported methods[6,7]. Analytical grade isopropanol (BDH Ltd) was refluxed with sodium and distilled before use in catalytic runs. Its purity was checked by gas chromatography. Nitrogen was purified by passing through a vanadium(II) solution and dried by passing through columns packed with anhydrous calcium chloride.

Apparatus and Methods

Differential thermal analysis (DTA) of iron and cobalt hydroxides and their mixtures was made with the use of an automatically recording thermobalance of the type 160 KS (Germany). The heating rate was 10 °C/min, and 20 mg of each solid specimen was used in each experiment. α-Alumina powder was applied as a DTA reference. X-Ray diffraction (XRD) analysis of the samples after their thermal treatment was made with the use of Philips diffractometer (Model PW 2103, 35 kV and 20 mA) with a source of CuKα radiation (Ni filtered). IR spectra of solid oxide catalysts were recorded in 1 600 – 200 cm^{-1} region with the spectrometer Perkin–Elmer, Model 599 B, using KBr technique. Adsorption–desorption N_2 isotherms were determined at −196 °C, after initial degassing of the catalysts at 150 °C for 1 h, using conventional volumetric apparatus[8]. The S_{BET} values were calculated from adsorption data using the linear form of the BET equation[9]. The porosity of the samples was assessed by the method of Brokhoff and de Boer[10,11]. The electrical conductivity measurements were made as described previously[12]. The catalytic reactions were carried out in a conventional fixed-bed flow type reactor. The exit feed was analyzed by direct sampling of the gaseous products into a Pye–Unicam gas chromatograph, determining the amount of isopropanol and its decomposition products. All the measurements were made after steady-state conditions were attained.

RESULTS AND DISCUSSION

Thermal Analysis

DTA curves of pure $Fe(OH)_3$, $Co(OH)_2$ and their mixtures are represented in Fig. 1. Curve *1* shows that the decomposition of $Fe(OH)_3$ proceeds in three steps with maxima

at 100, 240, and 500 °C, respectively. The first endothermic peak corresponds to the loss of the adsorbed water, while the second, less pronounced endothermic peak can be attributed to the hydroxide decomposition[13] to amorphous γ-Fe_2O_3. The third exothermic peak corresponds to the phase transition[14], i.e. γ-$Fe_2O_3 \rightarrow \alpha$-$Fe_2O_3$. On the addition of 0.2 or 0.4 mole % Co^{2+}, the exothermic peak located at 500 °C shifts to higher temperatures (577 and 604 °C, respectively), as shown by curves *2* and *3*. For $x = 0.6$, the just mentioned peak disappears while a small endothermic peak arises at around 660 °C (curve *4*). This new peak is due to the solid–solid interaction betweeen α-Fe_2O_3 and Co_3O_4, forming the spinel structure in the low concentration. On increasing x up to 1.5, the decomposition of these samples leads to a new exothermic peak with maximum at 410 °C and an endothermic peak located at 660 °C (curves *6* and *7* for $x = 1.0$ and 1.5, respectively). The former peak is caused by formation of cobalt–ferrite spinel[13] while the latter can be explained on the basis of cation distribution[15] via oxygen release. Further increase in Co^{2+} content (curves *8* – *13*) results in disappearance of two peaks at 410 and 660 °C. The area of the new endothermic peak at 930 – 960 °C increases with increasing x, reaching maximum for the pure $Co(OH)_2$. It can be attributed[16] to the phase transition of Co_3O_4 to CoO. On the other hand, the endothermic peak with maximum at 240 °C relates to the pure $Co(OH)_2$, and curve *13* is due to the decomposition[17] of $Co_2O_3 \cdot H_2O$ to Co_3O_4.

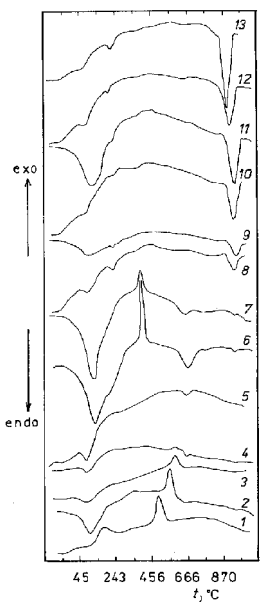

FIG. 1
DTA curves for iron hydroxide (*1*), cobalt hydroxide (*13*) and their mixtures containing cobalt hydroxide at ratios $x = 0.2$ (*2*), 0.4 (*3*), 0.6 (*4*), 0.8 (*5*), 1.0 (*6*), 1.5 (*7*), 2.0 (*8*), 2.2 (*9*), 2.4 (*10*), 2.6 (*11*), and 2.8 (*12*)

X-Ray Diffraction

To detect any chemical or structural change, all the prepared samples were subjected to X-ray analysis. The values obtained for the d-plane spacing and their relative intensities were matched with relevant ASTM cards[18]. The X-ray diffraction lines of the catalysts calcined at 600 °C for 3 h are represented in Fig. 2. The figure shows that the predominant diffraction lines corresponding to α-Fe_2O_3 (x = 0) are located at d (Å) = 2.63 (100), 2.44 (68), 1.67 (36) and 3.54 (34). The intensity of the diffraction line at d (Å) = 2.63 decreases on increasing Co^{2+} content and disappears at x = 1.0 whereas the line at d (Å) = 2.46 disappears on the addition of Co^{2+} at x = 0.6. On the other hand, the new lines at d (Å) = 2.51 (100), 1.48 (32), and 2.94 (30) reach maximum at x = 1.0 and can be attributed to the formation of $CoFe_2O_4$ lattice structure[15,19]. It is worth noting that the intensity of these lines decreases on increasing Co^{2+} content up to x = 2.4, then they disappear. Moreover, in the presence of Co^{2+} (x = 1.0), the lines corresponding to Co_3O_4 appear and become predominant at x = 2.2. The most intense lines corresponding to Co_3O_4 are located at d (Å) = 2.43 (100), 1.43 (53), 2.84 (45), 1.55 (44), 2.01 (30) and 4.62 (25). However, XRD results allow to conclude that $CoFe_2O_4$ spinel is formed in higher amounts at x = 1.0. Moreover, it predominates in the iron-rich region while its amount decreases sharply in the cobalt-rich region.

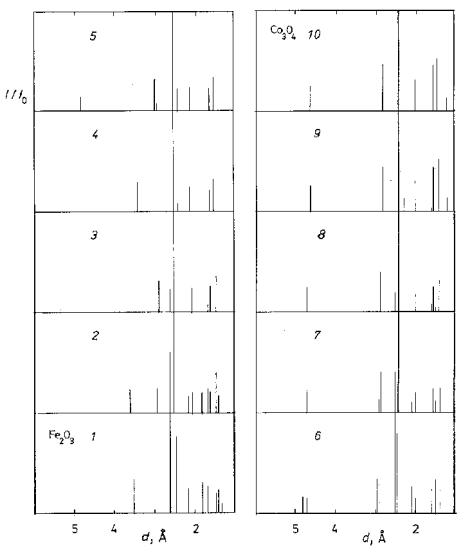

FIG. 2
XRD lines for iron oxide (Fe_2O_3) (*1*), cobalt oxide (Co_3O_4) (*10*) and their mixtures containing Co_3O_4 at ratios x = 0.6 (*2*), 0.8 (*3*), 1.0 (*4*), 1.5 (*5*), 2.0 (*6*), 2.2 (*7*), 2.4 (*8*), and 2.6 (*9*) calcined at 600 °C for 3 h in air

IR Spectra

Examination of IR spectra of the catalysts calcined at 600 °C for 3 h (Fig. 3), indicates that the absorption bands at 620 – 520, 460, 390, and 310 cm^{-1} correspond[20] to α-Fe_2O_3. On the other hand, the bands at 1 380, 660, 575 and 390 cm^{-1} could be assigned to Co_3O_4 lattice vibrations[20]. The absorption spectra of different spinel compositions (Fig. 3) have two strong broad bands located at 590 and 400 cm^{-1} for x = 0.6, 0.8, 1.0, 1.5, and 2.0. The bands observed for Co^{2+} content at $0.6 > x > 2.0$ correspond to the pure Fe_2O_3 and Co_3O_4. The first band was attributed to the intrinsic vibration of tetrahedral groups[21], whereas the second one was reported to be due to vibrations of the bivalent metal ion–oxygen complex[18].

Texture Assessment

The adsorption of nitrogen on the investigated catalysts proved to be rapid and reversible, yielding type II of BDDT classification[22]. The variations in texture of the catalysts calcined at 600 °C for 3 h were monitored for both pure and mixed oxides (Table I).

It is evident from Table I that S_{BET} of Fe_2O_3 increases on increasing Co^{2+} up to x = 0.6, then it decreases to x = 1.0. On the other hand, S_{BET} of Co_3O_4 increases with increasing Fe_2O_3 concentration up to x = 2.6, followed by continuous decrease to x = 2.0. The increase in S_{BET} of Fe_2O_3 on Co^{2+} addition can be attributed to the holes formed via incorporation of Co^{2+} into Fe_2O_3 lattice[23]. It is known that Co_3O_4 has the spinel structure which contains both CoO and Co_2O_3, Co^{2+} ions are only effective when incorporated into Fe_2O_3 lattice. Thus, the following equation can be suggested,

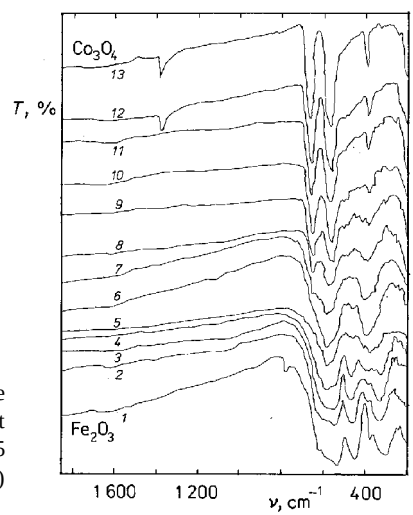

FIG. 3
IR spectra of iron oxide (Fe_2O_3) (*1*), cobalt oxide (Co_3O_4) (*13*), and their mixtures containing Co_3O_4 at ratios x = 0.2 (*2*), 0.4 (*3*), 0.6 (*4*), 0.8 (*5*), 1.0 (*6*), 1.5 (*7*), 2.0 (*8*), 2.2 (*9*), 2.4 (*10*), 2.6 (*11*), and 2.8 (*12*) calcined at 600 °C for 3 h in air

$$1/2\ O_2 + 2\ CoO \rightarrow 2\ Co|\ Fe\ |^{\prime} + Fe_2O_3 + 2\ |\ e\ |^{\cdot} \qquad (A)$$

where $Co|\ Fe\ |^{\prime}$ denotes Co^{2+} ions that replace Fe^{3+} ions in the normal lattice and $|\ e\ |^{\cdot}$ is a hole. Also, CoO could be partially incorporated in another way, such as

$$2\ CoO \rightarrow 2\ Co|\ Fe\ |^{\prime} + 1/2\ Fe_2O_3 + Fe^{3+} + 1/2\ O_2 + e \qquad (B)$$

where Fe^{3+} denotes interstitial ions leading to the lattice expansion accessible to nitrogen adsorption. On the other hand, the increase of S_{BET} of Co_3O_4 on the addition of Fe_2O_3 may be attributed to the Fe^{3+} incorporation into Co_3O_4 lattice, as shown in Eq. (*C*) where $Fe|\ Co\ |^{\prime}$ are Fe^{3+} ions substituting Co^{2+} ions in their normal sites.

$$Fe_2O_3 \rightarrow 2\ Fe|\ Co\ |^{\cdot} + 2\ CoO + 1/2\ O_2 + 2\ e \qquad (C)$$

TABLE I
Texture data for $Co_xFe_{3-x}O_4$ system calcined at 600 °C for 3 h in air

Co^{2+} Ratio x	S_{BET} m^2/g	S_t m^2/g	S_{cum} m^2/g	V_P cm^3/g	V_{Pcum} cm^3/g	S_t/S_{BET}
0[a]	7.06	7.0	8.1	0.02	0.05	0.991
0.2	16.8	16.7	20.8	0.06	0.11	0.994
0.4	22.7	22.6	21.6	0.06	0.09	0.991
0.6	25.8	23.8	18.3	0.06	0.12	0.992
0.8	22.9	22.8	31.0	0.10	0.13	0.996
1.0	9.1	8.3	10.9	0.02	0.03	0.912
1.5	10.5	10.4	17.1	0.06	0.10	0.991
2.0	9.7	9.6	13.7	0.04	0.07	0.990
2.2	20.4	19.9	26.6	0.09	0.15	0.976
2.4	27.1	27.0	30.4	0.08	0.12	0.996
2.6	31.6	29.3	36.4	0.08	0.12	0.918
2.8	19.0	19.0	25.7	0.07	0.12	1.000
3.0[b]	16.6	16.0	21.0	0.06	0.10	0.964

[a] Pure Fe_2O_3; [b] pure Co_3O_4.

The decrease in S_{BET} between two maxima may due to the starting formation of the spinel structure, as detected by X-ray diffraction. The noticable little variation in S_{BET} values at x = 1.0, 1.5, and 2.0 may be attributed to the formation of the normal spinel, i.e. $CoFe_2O_4$, which has stoichiometric structure[6]. However, the results suggest that formation of the normal spinel is accompanied with the low surface area.

The examination of the porosity of the catalyst (Table I) shows that when comparing S_{cum} with S_{BET} and V_{Pcum} with V_P, then $S_{cum} > S_{BET}$ and $V_{Pcum} > V_P$. This indicates a mesoporous nature. Similarly, also an upward deviation observed in the V_a–t plots is indicative of mesopores. Moreover, all the S_t/S_{BET} values are higher than 91%, which supports the validity of the standarded t-curve used.

Electrical Conductivity Measurements

Measurements of the electrical conductivity of Fe_2O_3, Co_3O_4 and their mixtures calcined at 600 °C for 3 h were carried out in the absence and presence of gaseous isopropanol at 325 °C. The variation of log σ with composition is shown in Fig. 4. Curve *1* indicates that in the absence of the alcohol (N_2 gas only), the addition of Co^{2+} into Fe_2O_3 lattice leads to conductance increase up to x = 0.4, then a small increase up to x = 2.2, followed by another increase up to x = 3.0. On the other hand, as the activation energy provides the better information on conductivity changes, the log σ values were plotted as a function of the reciprocal absolute temperature, and the activation energies (E_σ) were determined from the slopes of the obtained lines[24], where

$$\sigma = \sigma_0 \exp(-E_\sigma/\boldsymbol{R}T) \quad . \qquad (1)$$

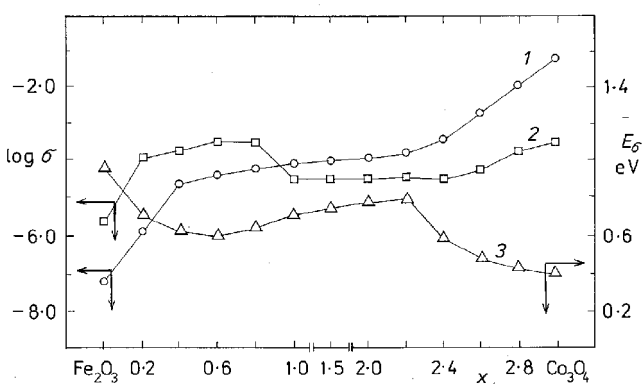

FIG. 4
The variation of log σ with composition of Fe_2O_3–Co_3O_4 system calcined at 600 °C for 3 h in the absence (*1*) and presence of isopropanol (*2*) and the activation energy E_σ (*3*) in nitrogen

The variation of the activation energy of electrical conduction with the catalyst composition is illustrated in Fig. 4, curve *3*. The results show that the conductance of Fe_2O_3 increases while the activation energy decreases on the addition of Co_3O_4 up to $x = 0.4$. It is known that the addition of Co_3O_4 (p-type, ref.[25]) to Fe_2O_3 (n-type, ref.[26]) should decrease the number of charge carriers and thus to decrease the electrical conductance. Our results indicate the opposite behaviour, which can be accounted for in terms of Eq. (*B*) if incorporation of Co^{2+} into Fe_2O_3 leads to generation of electrons. On the other hand, the addition of Fe_2O_3 to Co_3O_4 leads to a significant decrease in the conductance and an increase in E_σ. This may be explained on the basis of Eq. (*C*), the free electrons produced in p-type semiconductor decrease the number of charge carriers within the solid matrix, which decreases the conduction and, subsequently, it increases the activation energy. The conductance behaviour for x increasing up to 2.2 corresponds to the formation of the normal spinel $CoFe_2O_4$ spinel. Co^{2+} and Fe^{3+} cations are found to be unequally distributed among the tetrahedral and octahedral lattice, and the distribution is temperature-dependent[27]. As hopping between different cations on the octahedral sublattice[28] needs higher activation energy than for ions of the same metal, the conduction activation energy E_σ for the $CoFe_2O_4$ spinel is thus higher than that of the pure oxides, as shown in curve *3*. The higher values of E_σ may be due to the hopping stability between different valencies in the spinel structure. However, $Co_xFe_{3-x}O_4$ spinels have been studied by Jonker[29] who pointed out that the compositions with $1 \leq x \leq 3$ in this series are of p-type, whereas those with $0 \leq x \leq 1$ are n-type semiconductors. Moreover, iron rich oxides of this system are the inverse spinels[30], whereas the cobalt-rich ones are the normal spinels[31]. From the E_σ values presented in Fig. 4, curve *3*, one can conclude that in the iron-rich region the conductance increases and E_σ decreases, while the opposite behaviour is observed in the cobalt-rich region. Moreover, the region containing $CoFe_2O_4$ shows parallel change in conductance and activation energy.

The electrical conductivity changes of the catalysts were also measured in the presence of isopropanol vapours under the conditions of the catalytic decomposition of the alcohol (see later). The changes of log σ with time for the catalyst calcined at 600 °C for 3 h are shown in Fig. 5. In the iron-rich region, the steady state is attained after 30 min, whereas in the cobalt-rich region, the steady-state attainment is fast (ca 10 min). On the other hand, the region of maximum formation of the $CoFe_2O_4$ spinel (x = 1.0, 1.5, 2.0, and 2.2) shows little variation of conductance with time. These results describe the way by which electron exchange between the alcohol and the catalyst surface is realized. The log σ changes under steady-state conditions with catalyst compositions are shown in Fig. 4, curve *2*. They demonstrate the greater conductance during the reaction of isopropanol in the iron-rich region compared to the values obtained in the absence of the alcohol. Contrarily, the conductance of the solids in the cobalt-rich region and the region containing $CoFe_2O_4$ is lower than that obtained in the absence of isopropanol (curve *1*). The increase of conductance in the iron-rich region

lends further support to the n-type nature of the ferrite spinels and refers also to the transfer of electrons of the alcohol to the catalyst surface. It was reported that[32] the catalytic reaction of isopropanol on n-type solids increases the number of charge carriers, causing thus the increase of conductivity and the decrease of the activation energy, E_σ, while the opposite situation has been found for the conductivity of p-type. The decrease in the conductance of the samples with x above 0.8 can be attributed to the decrease of charge carriers via the consumption of the electrons released by isopropanol through the holes within the p-type semiconductors. This is in good agreement with the results reported by Jonker[29] and Dezsi[30]. In addition, the electronic theory of chemisorption on semiconducting solid materials[33] postulates a close relation between the electronic properties of a catalyst and its catalytic activity. The width of the energy gap is important in controlling the number of molecules which can be chemisorbed in the course of a catalytic reaction and the nature of the chemical bond formed between the molecule and the surface. These factors control at the same time the activity and selectivity of the catalyst as well as mechanism of the catalytic reaction.

Catalytic Activity

The catalytic decomposition of isopropanol over pure Fe_2O_3, Co_3O_4 and their mixtures calcined at 600 °C for 3 h was studied at 325 °C. The experimental conditions were W/F = 1.87 g cat mol/l h, 1.5% isopropanol, total flow rate = 150 ml/min NTP N_2 gas, and the steady state was established after 1 h. The conversion, yield and selectivity of the alcohol dehydration–dehydrogenation were calculated according to Agrawal et

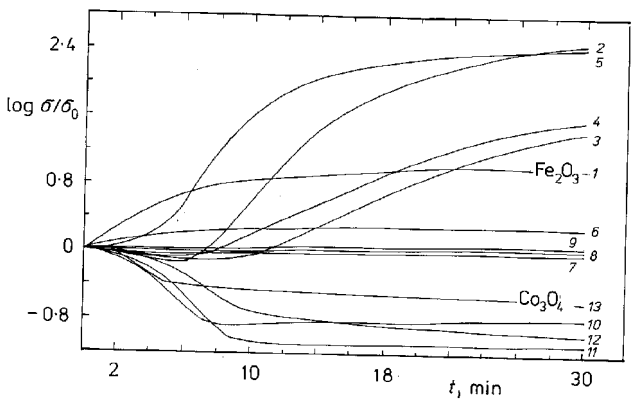

FIG. 5

Variation of log σ/σ_0 with time for iron oxide (Fe_2O_3) (*1*), cobalt oxide (Co_3O_4) (*13*) and their mixtures containing Co_3O_4 at ratios x = 0.2 (*2*), 0.4 (*3*), 0.6 (*4*), 0.8 (*5*), 1.0 (*6*), 1.5 (*7*), 2.0 (*8*), 2.2 (*9*), 2.4 (*10*), 2.6 (*11*) and 2.8 (*12*) calcined at 600 °C for 3 h during contact isopropanol at 325 °C

al.[34]. The results are shown in Fig. 6. It was found that acetone and propylene are the major products. The results can be divided into three groups: (i) when Fe_2O_3 contains Co^{2+} up to $x = 0.8$, the conversion and yields of acetone and propylene all increase. This increase, as already mentioned, is due to formation of the inverse spinel. The spinel[35,36] with $x < 1$ has the cation distribution, $[Fe^{3+}]_t[Fe^{2+}Co^{2+}Fe^{3+}]_oO_4$. Therefore, the existence of a redox couple in the inverse spinel within the octahedron is possible and facilitates chemisorption of isopropanol, and eventually also its decomposition. (ii) The great decrease in the conversion and yield of acetone on increasing Co^{2+} content up to $x = 1.0$ may be attributed to formation of the normal spinel $CoFe_2O_4$, accompanied with little electron exchange within its structure as $[Fe^{3+}]_t[Co^{2+}Fe^{3+}]_oO_4$. It is of interest that the great decrease in isopropanol conversion is accompanied by the great increase in the selectivity of this spinel with respect to propylene formation. This suggests that the reaction on $CoFe_2O_4$ proceeds mainly as dehydration. (iii) A steady increase in the conversion and yield of acetone above minimum on increasing Co^{2+} content up to $x = 2.6$ may be attributed to the conversion of the normal spinel into the inverse one. For $x > 1$ the chemical composition[35,36] of ferrites can be written as $[Fe^{3+}]_t[Co^{2+}Co^{3+}Fe^{3+}]_oO_4$. Conductivity of these samples in the absence of isopropanol (Fig. 4, curve *1*) indicates a continuous increase of their conductance. The increase in the conductivity of ferrite caused by replacement of Fe^{2+} ions in the octahedron with Co^{2+} cations in the spinel ferrite lattice can be attributed to the distribution of the entering cations over different sites in the spinel structure. Similar cation distribution in which Co^{2+}, Co^{3+} and Fe^{2+} ions occupy octahedral sites is also proposed[37] for the higher Co/Fe ratios, such as $[Fe^{3+}]_t[Co^{2+}Co^{3+}Fe^{2+}]_oO_4$.

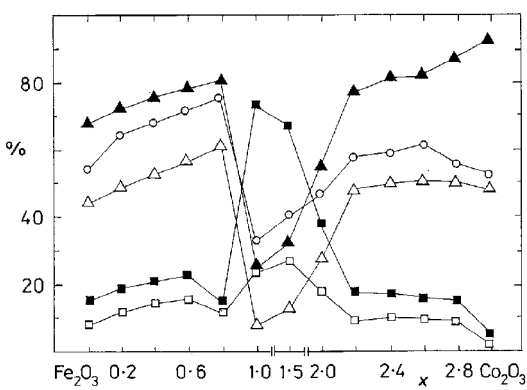

FIG. 6

Variation of isopropanol conversion (○), acetone yield (Δ), propylene yield (❒) and selectivity to acetone (▲) and to propylene (■) (all in %) with the catalyst composition (Fe_2O_3–Co_3O_4 system calcined at 600 °C for 3 h, the reaction carried out at 325 °C)

Such a distribution may lead to changes in both concentration and mobility of charge carriers in the ferrite lattice. Finally, the decrease in the conversion and acetone yield for the catalysts with x above 2.6 may be related to the activity of the cobalt oxide. XRD measurements indicated that the formation of the ferrite spinel decreases on increasing Co^{2+} content and disappears at $x = 2.6$. On the other hand, comparison of the activity and selectivity of the catalysts with conduction activation energies shows that on decreasing E_σ, the conversion, yield and selectivity towards acetone formation increases and vice versa. The decrease in E_σ should thus facilitate electron exchange between isopropanol and catalyst surface during the reaction.

In conclusion, the above results demonstrate that the dehydrogenation of isopropanol proceeds easily on the inverse spinel catalysts. The redox couple so formed is responsible for E_σ decrease, enhancing thus electron exchange between isopropanol and catalyst surface. Moreover, the inverse spinel in the iron-rich region is more active and selective with respect to acetone formation. On the other hand, the samples containing normal spinel exhibit low activity and selectivity in isopropanol decomposition.

REFERENCES

1. Goodenough J. B., Loelo A. L.: Phys. Rev. *98*, 391 (1955).
2. Hassan E. A., Abd El-Salaam K. M., Said A. A.: Bull. Chem. Soc. Jpn. *61*, 1331 (1988).
3. Onuchukwu A. I., Zuru A. B.: Math. Chem. Phys. *15*, 131 (1986).
4. Gabr R. M., Girgis M. M., El-Awad A. M.: Math. Chem. Phys. *28*, 413 (1991).
5. Rajaram R. R., Sermon P. A.: J. Chem. Soc., Faraday Trans. 1 *81*, 2577 (1985).
6. Tseung A. C. C., Goldstein J. R.: J. Phys. Chem. *76*, 3646 (1972).
7. Tseung A. C. C., Goldstein J. R.: J. Mater. Sci. *7*, 1383 (1972).
8. Kontro D. I., Brunauer S., Compeland L. E. in: *The Solid–Gas Interface* (A. Flood, Ed.), Vol. 1. Dekker, New York 1967.
9. Brunauer S., Emmett P. H., Teller E.: J. Am. Chem. Soc. *59*, 1533 (1938).
10. Brockoff J. C. P., de Boer J. H.: J. Catal. *9*, 15 (1967).
11. Brockoff J. C. P., de Boer J. H.: J. Catal. *10*, 153 (1967).
12. Said A. A., Hassan E. A., Abd El-Salaam K. M.: Surf. Technol. *20*, 123 (1983).
13. Barraga C. I., Lavela P., Morules J., Tirado J.: J. Colloid Interface Sci. *138*, 565 (1990).
14. Gillot B., Beneloucif R. M., Jammal F.: J. Mater. Sci. *19*, 3806 (1984).
15. Said A. A., Abd El-Salaam K. M., Hassan E. A., El-Awad A. M., Abd El-Wahab M. M. M.: J. Therm. Anal. *39*, 309 (1993).
16. Chisnall K. T., Lucas J. W., Sing K. S. W.: J. Appl. Chem. *15*, 358 (1965).
17. Figlarz M., Guenot J., Tournemolle J. N.: J. Mater. Sci. *19*, 772 (1974).
18. Blasse G.: Philips Res. Rep. *18*, 383 (1963).
19. Smith J. V. (Ed.): *X-Ray Powder Data File*. American Society for Testing Materials, Philadelphia 1960.
20. Nyquist R. A., Kagel R. O.: *Infrared Spectra of Inorganic Compounds*. Academic Press, London 1971.
21. Waldron R. D.: Phys. Rev. *99*, 1727 (1955).
22. Brunauer S., Deming L. S., Deming W. S., Teller E.: J. Am. Chem. Soc. *62*, 1723 (1940).
23. Abd El-Salaam K. M., Hassan E. A., Said A. A.: Adsorption Sci. Tech. *1*, 169 (1984).

24. Morrison S. R.: *Chemical Physics of Surfaces*, p. 70. Plenum, New York 1977.
25. Slack G.: J. Appl. Phys. *31*, 157 (1960).
26. Neel L.: Ann. Phys. (France) *3*, 137 (1948).
27. Sawatzky G. A., Vanderwoude F., Horish A. H.: Phys. Rev. *187*, 747 (1969).
28. Wu C. C., Kumarakrishnan S., Mason T. O.: J. Solid State Chem. *37*, 144 (1981).
29. Jonker G. H.: J. Phys. Chem. Solids *9*, 165 (1965).
30. Dezsi I.: Acta Phys. Pol. *24*, 283 (1963).
31. Lotgering F. K.: Phillips Res. Reports *11*, 337 (1956).
32. Abd El-Salaam K. M., Said A. A.: Oxid. Commun. *3*, 291 (1984).
33. Hauffe K.: Adv. Catal. *7*, 213 (1955).
34. Agrawal D. C., Nigam P. C., Srivastava R. D.: J. Catal. *55*, 1 (1978).
35. Gillot B., Benloucif R. M., Rousset A.: Mater. Res. Bull. *16*, 481 (1981).
36. Rousset A., Mollard P., Giraud A.: C. R. Acad. Sci. *275*, 709 (1972).
37. Gillot B., Jammal F.: Phys. Status Solidi, A *67*, 601 (1983).

Translation revised by J. Hetflejs.